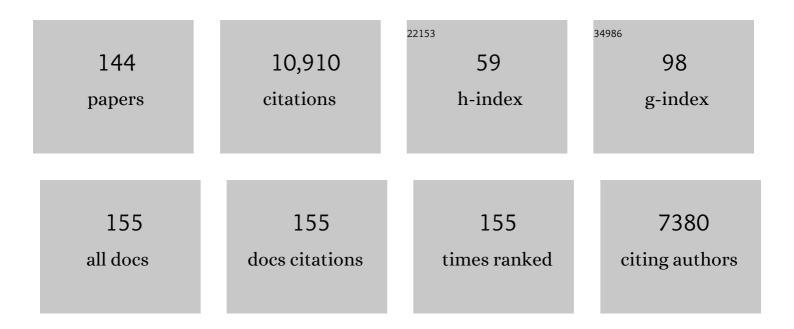
Klaus Wallmann

List of Publications by Year in descending order

Source: https://exaly.com/author-pdf/3255182/publications.pdf Version: 2024-02-01



#	Article	IF	CITATIONS
1	Gas hydrate destabilization: enhanced dewatering, benthic material turnover and large methane plumes at the Cascadia convergent margin. Earth and Planetary Science Letters, 1999, 170, 1-15.	4.4	386
2	Fluid flow, methane fluxes, carbonate precipitation and biogeochemical turnover in gas hydrate-bearing sediments at Hydrate Ridge, Cascadia Margin: numerical modeling and mass balances. Geochimica Et Cosmochimica Acta, 2003, 67, 3403-3421.	3.9	329
3	Anaerobic oxidation of methane above gas hydrates at Hydrate Ridge, NE Pacific Ocean. Marine Ecology - Progress Series, 2003, 264, 1-14.	1.9	296
4	The oxygen isotope evolution of seawater: A critical review of a long-standing controversy and an improved geological water cycle model for the past 3.4Âbillion years. Earth-Science Reviews, 2007, 83, 83-122.	9.1	295
5	Gas hydrate growth, methane transport, and chloride enrichment at the southern summit of Hydrate Ridge, Cascadia margin off Oregon. Earth and Planetary Science Letters, 2004, 226, 225-241.	4.4	264
6	Controls on the cretaceous and cenozoic evolution of seawater composition, atmospheric CO 2 and climate. Geochimica Et Cosmochimica Acta, 2001, 65, 3005-3025.	3.9	250
7	Rising Arctic Ocean temperatures cause gas hydrate destabilization and ocean acidification. Geophysical Research Letters, 2011, 38, n/a-n/a.	4.0	247
8	The Global Inventory of Methane Hydrate in Marine Sediments: A Theoretical Approach. Energies, 2012, 5, 2449-2498.	3.1	240
9	Early diagenesis of redox-sensitive trace metals in the Peru upwelling area – response to ENSO-related oxygen fluctuations in the water column. Geochimica Et Cosmochimica Acta, 2011, 75, 7257-7276.	3.9	223
10	Fluid expulsion related to mud extrusion off Costa Rica—A window to the subducting slab. Geology, 2004, 32, 201.	4.4	221
11	Calcium isotope record of Phanerozoic oceans: Implications for chemical evolution of seawater and its causative mechanisms. Geochimica Et Cosmochimica Acta, 2007, 71, 5117-5134.	3.9	211
12	Calculation of the stability and solubility of methane hydrate in seawater. Chemical Geology, 2005, 219, 37-52.	3.3	210
13	Paleoclimates, ocean depth, and the oxygen isotopic composition of seawater. Earth and Planetary Science Letters, 2006, 252, 82-93.	4.4	205
14	Silicate weathering in anoxic marine sediments. Geochimica Et Cosmochimica Acta, 2008, 72, 2895-2918.	3.9	194
15	The geological water cycle and the evolution of marine \hat{I} 18 O values. Geochimica Et Cosmochimica Acta, 2001, 65, 2469-2485.	3.9	189
16	Early diagenetic processes, fluxes, and reaction rates in sediments of the South Atlantic. Geochimica Et Cosmochimica Acta, 1994, 58, 2041-2060.	3.9	184
17	Kinetics of organic matter degradation, microbial methane generation, and gas hydrate formation in anoxic marine sediments. Geochimica Et Cosmochimica Acta, 2006, 70, 3905-3927.	3.9	181
18	Numerical modeling of carbonate crust formation at cold vent sites: significance for fluid and methane budgets and chemosynthetic biological communities. Earth and Planetary Science Letters, 2004, 221, 337-353.	4.4	178

KLAUS WALLMANN

#	Article	IF	CITATIONS
19	Rising methane gas bubbles form massive hydrate layers at the seafloor. Geochimica Et Cosmochimica Acta, 2004, 68, 4335-4345.	3.9	162
20	Hydrogeological system of erosional convergent margins and its influence on tectonics and interplate seismogenesis. Geochemistry, Geophysics, Geosystems, 2008, 9, .	2.5	159
21	Constraining the marine strontium budget with natural strontium isotope fractionations (87Sr/86Srâ^—,) Tj ETQq1 2010, 74, 4097-4109.	l 1 0.7843 3.9	514 rgBT /○ 154
22	Nucleation of calcium carbonate on bacterial nanoglobules. Geology, 2006, 34, 1017.	4.4	151
23	Dissolution kinetics of biogenic silica from the water column to the sediments. Geochimica Et Cosmochimica Acta, 2002, 66, 439-455.	3.9	147
24	Estimation of the global inventory of methane hydrates in marine sediments using transfer functions. Biogeosciences, 2013, 10, 959-975.	3.3	145
25	Quantifying fluid flow, solute mixing, and biogeochemical turnover at cold vents of the eastern Aleutian subduction zone. Geochimica Et Cosmochimica Acta, 1997, 61, 5209-5219.	3.9	143
26	Estimation of the global amount of submarine gas hydrates formed via microbial methane formation based on numerical reaction-transport modeling and a novel parameterization of Holocene sedimentation. Geochimica Et Cosmochimica Acta, 2011, 75, 4562-4576.	3.9	143
27	Benthic iron and phosphorus fluxes across the Peruvian oxygen minimum zone. Limnology and Oceanography, 2012, 57, 851-867.	3.1	130
28	A revised global estimate of dissolved iron fluxes from marine sediments. Global Biogeochemical Cycles, 2015, 29, 691-707.	4.9	126
29	Fluid venting in the eastern Aleutian Subduction Zone. Journal of Geophysical Research, 1998, 103, 2597-2614.	3.3	123
30	Cretaceous and Cenozoic evolution of seawater composition, atmospheric O2 and CO2: A model perspective. Numerische Mathematik, 2003, 303, 94-148.	1.4	111
31	Atlantic cooling associated with a marine biotic crisis during the mid-Cretaceous period. Nature Geoscience, 2013, 6, 558-561.	12.9	110
32	The Phanerozoic δ88/86Sr record of seawater: New constraints on past changes in oceanic carbonate fluxes. Geochimica Et Cosmochimica Acta, 2014, 128, 249-265.	3.9	101
33	The effect of dissolved barium on biogeochemical processes at cold seeps. Geochimica Et Cosmochimica Acta, 2004, 68, 1735-1748.	3.9	100
34	Feedbacks between oceanic redox states and marine productivity: A model perspective focused on benthic phosphorus cycling. Global Biogeochemical Cycles, 2003, 17, n/a-n/a.	4.9	98
35	Gas hydrate dissociation off Svalbard induced by isostatic rebound rather than global warming. Nature Communications, 2018, 9, 83.	12.8	97
36	New procedure for determining reactive Fe(III) and Fe(II) minerals in sediments. Limnology and Oceanography, 1993, 38, 1803-1812.	3.1	96

KLAUS WALLMANN

#	Article	IF	CITATIONS
37	Fluid venting activity on the Costa Rica margin: new results from authigenic carbonates. International Journal of Earth Sciences, 2004, 93, 596.	1.8	96
38	Distribution, biomass and diversity of benthic foraminifera in relation to sediment geochemistry in the Arabian Sea. Deep-Sea Research Part II: Topical Studies in Oceanography, 2000, 47, 2913-2955.	1.4	94
39	Calcium isotope (δ44/40Ca) variations of Neogene planktonic foraminifera. Paleoceanography, 2005, 20, n/a-n/a.	3.0	94
40	Vodyanitskii mud volcano, Sorokin trough, Black Sea: Geological characterization and quantification of gas bubble streams. Marine and Petroleum Geology, 2009, 26, 1799-1811.	3.3	93
41	Methane discharge into the Black Sea and the global ocean via fluid flow through submarine mud volcanoes. Earth and Planetary Science Letters, 2006, 248, 545-560.	4.4	92
42	Benthic nitrogen cycling traversing the Peruvian oxygen minimum zone. Geochimica Et Cosmochimica Acta, 2011, 75, 6094-6111.	3.9	90
43	Iron species determination to investigate early diagenetic reactivity in marine sediments. Geochimica Et Cosmochimica Acta, 1997, 61, 63-72.	3.9	89
44	Bubble-induced porewater mixing: A 3-D model for deep porewater irrigation. Geochimica Et Cosmochimica Acta, 2007, 71, 5135-5154.	3.9	89
45	Cold seeps along the main Marmara Fault in the Sea of Marmara (Turkey). Deep-Sea Research Part I: Oceanographic Research Papers, 2008, 55, 552-570.	1.4	86
46	Structure and thermal expansion of natural gas clathrate hydrates. Chemical Engineering Science, 2006, 61, 2670-2674.	3.8	85
47	Organic carbon production, mineralisation and preservation on the Peruvian margin. Biogeosciences, 2015, 12, 1537-1559.	3.3	81
48	Stable silicon isotope signatures of marine pore waters – Biogenic opal dissolution versus authigenic clay mineral formation. Geochimica Et Cosmochimica Acta, 2016, 191, 102-117.	3.9	80
49	In situ benthic fluxes from an intermittently active mud volcano at the Costa Rica convergent margin. Earth and Planetary Science Letters, 2005, 235, 79-95.	4.4	78
50	Permian–Triassic mass extinction pulses driven by major marine carbon cycle perturbations. Nature Geoscience, 2020, 13, 745-750.	12.9	78
51	Phosphorus imbalance in the global ocean?. Global Biogeochemical Cycles, 2010, 24, .	4.9	75
52	Methane hydrate accumulation in "Mound 11―mud volcano, Costa Rica forearc. Marine Geology, 2005, 216, 83-100.	2.1	74
53	Artifacts in the Determination of Trace Metal Binding Forms in Anoxic Sediments by Sequential Extraction. International Journal of Environmental Analytical Chemistry, 1993, 51, 187-200.	3.3	73
54	Methane-Carbon Flow into the Benthic Food Web at Cold Seeps – A Case Study from the Costa Rica Subduction Zone. PLoS ONE, 2013, 8, e74894.	2.5	70

#	Article	IF	CITATIONS
55	Quantification of methane emissions at abandoned gas wells in the Central North Sea. Marine and Petroleum Geology, 2015, 68, 848-860.	3.3	69
56	Salty brines on the Mediterranean sea floor. Nature, 1997, 387, 31-32.	27.8	68
57	Fluid expulsion from the Dvurechenskii mud volcano (Black Sea)Part I. Fluid sources and relevance to Li, B, Sr, I and dissolved inorganic nitrogen cycles. Earth and Planetary Science Letters, 2004, 225, 347-363.	4.4	66
58	Silicate weathering in anoxic marine sediment as a requirement for authigenic carbonate burial. Earth-Science Reviews, 2020, 200, 102960.	9.1	65
59	Methane formation at Costa Rica continental margin—constraints for gas hydrate inventories and cross-décollement fluid flow. Earth and Planetary Science Letters, 2005, 236, 41-60.	4.4	63
60	Simulation of long-term feedbacks from authigenic carbonate crust formation at cold vent sites. Chemical Geology, 2005, 216, 157-174.	3.3	62
61	Numerical modeling of benthic processes in the deep Arabian Sea. Deep-Sea Research Part II: Topical Studies in Oceanography, 2000, 47, 3039-3072.	1.4	61
62	Factors influencing the distribution of epibenthic megafauna across the Peruvian oxygen minimum zone. Deep-Sea Research Part I: Oceanographic Research Papers, 2012, 68, 123-135.	1.4	61
63	Remobilization events involving Cd and Zn from intertidal flat sediments in the elbe estuary during the tidal cycle. Estuarine, Coastal and Shelf Science, 1992, 35, 371-393.	2.1	59
64	Relating sulfate and methane dynamics to geology: Accretionary prism offshore SW Taiwan. Geochemistry, Geophysics, Geosystems, 2013, 14, 2523-2545.	2.5	57
65	Modeling benthic–pelagic nutrient exchange processes and porewater distributions in a seasonally hypoxic sediment: evidence for massive phosphate release by <i>Beggiatoa</i> ?. Biogeosciences, 2013, 10, 629-651.	3.3	57
66	Impact of atmospheric CO2and galactic cosmic radiation on Phanerozoic climate change and the marine δ180 record. Geochemistry, Geophysics, Geosystems, 2004, 5, .	2.5	56
67	Simulating the biogeochemical effects of volcanic CO2 degassing on the oxygen-state of the deep ocean during the Cenomanian/Turonian Anoxic Event (OAE2). Earth and Planetary Science Letters, 2011, 305, 371-384.	4.4	55
68	Simple transfer functions for calculating benthic fixed nitrogen losses and C:N:P regeneration ratios in global biogeochemical models. Global Biogeochemical Cycles, 2012, 26, .	4.9	55
69	Consequences of moderate â^1⁄425,000Âyr lasting emission of light CO2 into the mid-Cretaceous ocean. Earth and Planetary Science Letters, 2007, 259, 200-211.	4.4	52
70	Sources of fluids and gases expelled at cold seeps offshore Georgia, eastern Black Sea. Geochimica Et Cosmochimica Acta, 2011, 75, 3250-3268.	3.9	52
71	Isotopic evidence (He, B, C) for deep fluid and mud mobilization from mud volcanoes in the Caucasus continental collision zone. International Journal of Earth Sciences, 2003, 92, 407-425.	1.8	50
72	Benthic nitrogen fluxes and fractionation of nitrate in the Mauritanian oxygen minimum zone (Eastern Tropical North Atlantic). Geochimica Et Cosmochimica Acta, 2014, 134, 234-256.	3.9	49

#	Article	IF	CITATIONS
73	Fluid flow through active mud dome Mound Culebra offshore Nicoya Peninsula, Costa Rica: evidence from heat flow surveying. Marine Geology, 2004, 207, 145-157.	2.1	48
74	Rates and regulation of nitrogen cycling in seasonally hypoxic sediments during winter (Boknis Eck,) Tj ETQqO 14-28.	0 0 rgBT /C 2.1	overlock 10 Tf 47
75	Carbon isotope exchange during anaerobic oxidation of methane (AOM) in sediments of the northeastern South China Sea. Geochimica Et Cosmochimica Acta, 2019, 246, 138-155.	3.9	47
76	Intercalibration of Bruevich's method to determine the total alkalinity in seawater. Oceanology, 2008, 48, 438-443.	1.2	46
77	The physicochemical habitat of <i>Sclerolinum</i> sp. at Hook Ridge hydrothermal vent, Bransfield Strait, Antarctica. Limnology and Oceanography, 2005, 50, 598-606.	3.1	45
78	Controls on authigenic carbonate precipitation at cold seeps along the convergent margin off Costa Rica. Geochemistry, Geophysics, Geosystems, 2010, 11, .	2.5	43
79	Evidence for the submarine weathering of silicate minerals in Black Sea sediments: Possible implications for the marine Li and B cycles. Geochemistry, Geophysics, Geosystems, 2004, 5, n/a-n/a.	2.5	41
80	Chemical, biological and hydrological controls on the 14C content of cold seep carbonate crusts: numerical modeling and implications for convection at cold seeps. Chemical Geology, 2004, 213, 359-383.	3.3	41
81	Pore-water distribution and quantification of diffusive benthic fluxes of silicic acid, nitrate and phosphate in surface sediments of the deep Arabian Sea. Deep-Sea Research Part II: Topical Studies in Oceanography, 2000, 47, 2707-2734.	1.4	39
82	The influence of volcanic ash alteration on the REE composition of marine pore waters. Journal of Geochemical Exploration, 2010, 106, 176-187.	3.2	39
83	A model for microbial phosphorus cycling in bioturbated marine sediments: Significance for phosphorus burial in the early Paleozoic. Geochimica Et Cosmochimica Acta, 2016, 189, 251-268.	3.9	38
84	Robust and fast FORTRAN and MATLAB® libraries to calculate pH distributions in marine systems. Computers and Geosciences, 2001, 27, 157-169.	4.2	36
85	Biological nitrate transport in sediments on the Peruvian margin mitigates benthic sulfide emissions and drives pelagic N loss during stagnation events. Deep-Sea Research Part I: Oceanographic Research Papers, 2016, 112, 123-136.	1.4	36
86	3â€D basinâ€scale reconstruction of natural gas hydrate system of the <scp>G</scp> reen <scp>C</scp> anyon, <scp>G</scp> ulf of <scp>M</scp> exico. Geochemistry, Geophysics, Geosystems, 2017, 18, 1959-1985.	2.5	36
87	Stable sulfur isotopes indicate net sulfate reduction in near-surface sediments of the deep Arabian Sea. Deep-Sea Research Part II: Topical Studies in Oceanography, 2000, 47, 2769-2783.	1.4	34
88	Hot vents in an ice-cold ocean: Indications for phase separation at the southernmost area of hydrothermal activity, Bransfield Strait, Antarctica. Earth and Planetary Science Letters, 2001, 193, 381-394.	4.4	34
89	Cool episodes in the Cretaceous $\hat{a} \in$ " Exploring the effects of physical forcings on Antarctic snow accumulation. Earth and Planetary Science Letters, 2011, 307, 279-288.	4.4	33
90	Footprint and detectability of a well leaking CO2 in the Central North Sea: Implications from a field experiment and numerical modelling. International Journal of Greenhouse Gas Control, 2019, 84, 190-203.	4.6	33

KLAUS WALLMANN

#	Article	IF	CITATIONS
91	Volcanogenic sediment–seawater interactions and the geochemistry of pore waters. Chemical Geology, 2008, 249, 321-338.	3.3	32
92	Pathways and regulation of carbon, sulfur and energy transfer in marine sediments overlying methane gas hydrates on the Opouawe Bank (New Zealand). Geochimica Et Cosmochimica Acta, 2010, 74, 5763-5784.	3.9	32
93	Estimating the time of pockmark formation in the SW Xisha Uplift (South China Sea) using reaction-transport modeling. Marine Geology, 2015, 364, 21-31.	2.1	32
94	Hydrothermal activity at Hook Ridge in the Central Bransfield Basin, Antarctica. Geo-Marine Letters, 1998, 18, 277-284.	1.1	31
95	Origin of salt-enriched pore fluids in the northern Gulf of Mexico. Earth and Planetary Science Letters, 2007, 259, 266-282.	4.4	31
96	A 35-million-year record of seawater stable Sr isotopes reveals a fluctuating global carbon cycle. Science, 2021, 371, 1346-1350.	12.6	31
97	Sedimentation and formation of secondary minerals in the hypersaline Discovery Basin, eastern Mediterranean. Marine Geology, 2002, 186, 9-28.	2.1	29
98	Halogen and ¹²⁹ I systematics in gas hydrate fields at the northern Cascadia margin (IODP) Tj ETQc	0 Q Q rgBT 2.5 rgBT	[/Qyerlock 10
99	3-D numerical modelling of methane hydrate accumulations using PetroMod. Marine and Petroleum Geology, 2016, 71, 288-295.	3.3	29
100	Benthic phosphorus cycling in the Peruvian oxygen minimum zone. Biogeosciences, 2016, 13, 1367-1386.	3.3	27
101	Cretaceous oceanic anoxic events prolonged by phosphorus cycle feedbacks. Climate of the Past, 2020, 16, 757-782.	3.4	27
102	The contribution of organic matter to the alkaline reserve of natural waters. Oceanology, 2006, 46, 192-199.	1.2	26
103	A transfer function for the prediction of gas hydrate inventories in marine sediments. Biogeosciences, 2010, 7, 2925-2941.	3.3	26
104	Impact of ambient conditions on the Si isotope fractionation in marine pore fluids during early diagenesis. Biogeosciences, 2020, 17, 1745-1763.	3.3	26
105	Geochemistry of gas hydrate accumulation offshore NE Sakhalin Island (the Sea of Okhotsk): results from the KOMEX-2002 cruise. Geo-Marine Letters, 2003, 23, 278-288.	1.1	25
106	The thermal structure of the Dvurechenskii mud volcano and its implications for gas hydrate stability and eruption dynamics. Marine and Petroleum Geology, 2009, 26, 1812-1823.	3.3	25
107	Serpentine alteration as source of high dissolved silicon and elevated δ30Si values to the marine Si cycle. Nature Communications, 2020, 11, 5123.	12.8	24
108	Development, test, and evaluation of exploitation technologies for the application of gas production from natural gas hydrate reservoirs and their potential application in the Danube Delta, Black Sea. Marine and Petroleum Geology, 2020, 120, 104488.	3.3	23

#	Article	IF	CITATIONS
109	Freshening of the Marmara Sea prior to its post-glacial reconnection to the Mediterranean Sea. Earth and Planetary Science Letters, 2015, 413, 176-185.	4.4	22
110	Effects of eustatic sea-level change, ocean dynamics, and nutrient utilization on atmospheric <i>p</i> CO ₂ and seawater composition over the last 130†000 years: a model study. Climate of the Past, 2016, 12, 339-375.	3.4	22
111	Shallow Gas Migration along Hydrocarbon Wells–An Unconsidered, Anthropogenic Source of Biogenic Methane in the North Sea. Environmental Science & Technology, 2017, 51, 10262-10268.	10.0	21
112	Recycling and Burial of Biogenic Silica in an Open Margin Oxygen Minimum Zone. Global Biogeochemical Cycles, 2021, 35, e2020GB006583.	4.9	21
113	Controls on organic carbon and molybdenum accumulation in Cretaceous marine sediments from the Cenomanian–Turonian interval including Oceanic Anoxic Event 2. Chemical Geology, 2012, 324-325, 28-45.	3.3	20
114	Strong and Dynamic Benthic-Pelagic Coupling and Feedbacks in a Coastal Upwelling System (Peruvian) Tj ETQq0	0 0 rgBT /	Overlock 10
115	Origin and Transformation of Light Hydrocarbons Ascending at an Active Pockmark on Vestnesa Ridge, Arctic Ocean. Journal of Geophysical Research: Solid Earth, 2020, 125, e2018JB016679.	3.4	20
116	Simulating and Quantifying Multiple Natural Subsea CO ₂ Seeps at Panarea Island (Aeolian) Tj ETQq Science & Technology, 2019, 53, 10258-10268.	0 0 0 rgBT 10.0	/Overlock 10 19
117	Studies on the adsorption of cadmium on hydrous iron(III) oxides in oxic sediments. Analytica Chimica Acta, 1993, 273, 323-327.	5.4	18
118	Phanerozoic evolution of atmospheric methane. Global Biogeochemical Cycles, 2008, 22, .	4.9	18
119	In Situ Temperature Measurements at the Svalbard Continental Margin: Implications for Gas Hydrate Dynamics. Geochemistry, Geophysics, Geosystems, 2018, 19, 1165-1177.	2.5	18
120	Oxygen minimum zone-type biogeochemical cycling in the Cenomanian-Turonian Proto-North Atlantic across Oceanic Anoxic Event 2. Earth and Planetary Science Letters, 2019, 517, 50-60.	4.4	18
121	Distribution and accumulation rate of Hg in the upper quaternary sediments of the Deryugin Basin, Sea of Okhotsk. Geochemistry International, 2007, 45, 47-61.	0.7	17
122	Is late Quaternary climate change governed by self-sustained oscillations in atmospheric CO2?. Geochimica Et Cosmochimica Acta, 2014, 132, 413-439.	3.9	17
123	Periodic changes in the Cretaceous ocean and climate caused by marine redox see-saw. Nature Geoscience, 2019, 12, 456-461.	12.9	17
124	lsotopic fingerprints of benthic nitrogen cycling in the Peruvian oxygen minimum zone. Geochimica Et Cosmochimica Acta, 2019, 245, 406-425.	3.9	15
125	Dissolved benthic phosphate, iron and carbon fluxes in the Mauritanian upwelling system and implications for ongoing deoxygenation. Deep-Sea Research Part I: Oceanographic Research Papers, 2019, 143, 70-84.	1.4	15
126	Formation pathways of light hydrocarbons in deep sediments of the Danube deep-sea fan, Western Black Sea. Marine and Petroleum Geology, 2020, 122, 104627.	3.3	14

#	Article	IF	CITATIONS
127	Constraining Global Marine Iron Sources and Ligandâ€Mediated Scavenging Fluxes With GEOTRACES Dissolved Iron Measurements in an Ocean Biogeochemical Model. Global Biogeochemical Cycles, 2021, 35, e2021GB006948.	4.9	14
128	Title is missing!. Earth and Planetary Science Letters, 2004, 225, 347-363.	4.4	13
129	Reply to comment on: "Gas hydrate growth, methane transport and chloride enrichment at the southern summit of Hydrate Ridge, Cascadia Margin off Oregon― Earth and Planetary Science Letters, 2005, 239, 168-175.	4.4	12
130	Quantification of methane emission from bacterial mat sites at Quepos Slide offshore Costa Rica. International Journal of Earth Sciences, 2014, 103, 1817-1829.	1.8	9
131	Genesis of mud volcano fluids in the Gulf of Cadiz using a novel basin-scale model approach. Geochimica Et Cosmochimica Acta, 2018, 243, 186-204.	3.9	9
132	Ocean phosphorus inventory: large uncertainties in future projections on millennial timescales and their consequences for ocean deoxygenation. Earth System Dynamics, 2019, 10, 539-553.	7.1	9
133	Interactions between deep formation fluid and gas hydrate dynamics inferred from pore fluid geochemistry at active pockmarks of the Vestnesa Ridge, west Svalbard margin. Marine and Petroleum Geology, 2021, 127, 104957.	3.3	9
134	Quantification of dissolved CO2 plumes at the Goldeneye CO2-release experiment. International Journal of Greenhouse Gas Control, 2021, 109, 103387.	4.6	9
135	Sediment release of dissolved organic matter to the oxygen minimum zone off Peru. Biogeosciences, 2020, 17, 4663-4679.	3.3	9
136	Solubility of cadmium and cobalt in a post-oxic or sub-oxic sediment suspension. Hydrobiologia, 1992, 235-236, 611-622.	2.0	8
137	Old iodine in fluids venting along the Central American convergent margin. Geophysical Research Letters, 2007, 34, .	4.0	8
138	Oil and gas seepage offshore Georgia (Black Sea) – Geochemical evidences for a paleogene-neogene hydrocarbon source rock. Marine and Petroleum Geology, 2021, 128, 104995.	3.3	8
139	Biogeochemical feedbacks may amplify ongoing and future ocean deoxygenation: a case study from the Peruvian oxygen minimum zone. Biogeochemistry, 2022, 159, 45-67.	3.5	8
140	Geochemical characterization of deep-sea sediments on the Azores Plateau – From diagenesis to hydrothermal activity. Marine Geology, 2020, 429, 106291.	2.1	7
141	Liverworts and all. Nature Geoscience, 2008, 1, 14-15.	12.9	5
142	The Influence of Diagenetic Processes on the Exchange of Trace Contaminants at the Sediment-Water Interface. , 1996, , 37-50.		3
143	Origin of High Mg and SO 4 Fluids in Sediments of the Terceira Rift, Azoresâ€Indications for Caminite Dissolution in a Waning Hydrothermal System. Geochemistry, Geophysics, Geosystems, 2019, 20, 6078-6094.	2.5	3
144	Effects of Ca-enrichment on authigenic carbonate formation at cold vent sites off Costa Rica: a numerical model approach. Mineralogical Magazine, 2008, 72, 325-327.	1.4	0